Received: 3 April 2019 | Revised: 25 June 2019 | Accepted: 13 July 2019

DOI: 10.1002/hbm.24735

RESEARCH ARTICLE

Close yet independent: Dissociation of social from valence and abstract semantic dimensions in the left anterior temporal lobe

Xiaosha Wang[1,2] | Bijun Wang[1,2] | Yanchao Bi[1,2]

[1]State Key Laboratory of Cognitive Neuroscience and Learning & IDG/McGovern Institute for Brain Research, Beijing Normal University, Beijing, China

[2]Beijing Key Laboratory of Brain Imaging and Connectomics, Beijing Normal University, Beijing, China

Correspondence
Yanchao Bi, State Key Laboratory of Cognitive Neuroscience and Learning & IDG/McGovern Institute for Brain Research, Beijing Normal University, Beijing 100875, China.
Email: ybi@bnu.edu.cn

Funding information
China Postdoctoral Science Foundation, Grant/Award Number: 2017M610791; Fundamental Research Funds for the Central Universities, Grant/Award Number: 2017EYT35; the 111 Project, Grant No. BP0719032; National Natural Science Foundation of China, Grant/Award Numbers: 31671128, 31700943; National Program for Special Support of Top-notch Young Professionals; the Changjiang Scholar Professorship Award, Grant/Award Number: T2016031

Abstract

The anterior temporal lobe (ATL) is engaged in various types of semantic dimensions. One consistently reported dimension is social information, with abstract words describing social behaviors inducing stronger activations in the ATL than nonsocial words. One potential factor that has been systematically confounded in this finding is emotional valence, given that abstract social words tend to be associated with emotional feelings. We investigated which factors drove the ATL sensitivity using a 2 (social/nonsocial) × 2 (valenced/neutral) factorial design in an fMRI study with relatively high spatial resolutions. We found that sociality and valence were processed in different ATL regions without significant interactions: The social effect was found in the left anterior superior temporal sulcus (aSTS), whereas the valence effect activated small clusters in the bilateral temporal poles (TP). In the left ATL, the social- and valence-related clusters were distinct from another superior ATL area that exhibited a general "abstractness" effect with little modulation of sociality or valence. These subregions exhibited distinct whole-brain functional connectivity patterns during the resting state, with the social cluster functionally connected to the default mode network, the valence cluster connected to the adjacent temporal regions and amygdala, and the abstractness cluster connected to a distributed network including a set of language-related regions. These results of activation profiles and connectivity patterns together indicate that the way in which the left ATL supports semantic processing is highly fine-grained, with the neural substrate for social semantic effects dissociated from those for emotional valence and abstractness.

KEYWORDS
abstract words, anterior temporal lobe, emotional valence, semantics, sociality

1 | INTRODUCTION

Our conceptual knowledge of the world around us, including objects, events, and abstract thoughts, lays the foundation for our daily behaviors. How such knowledge is stored and processed in the human brain has been extensively studied in the past few decades. Accumulating evidence shows that distributed, dissociable brain areas support different types of knowledge, such as animate versus inanimate objects, abstract versus concrete concepts, and social versus nonsocial words (Simmons, Reddish, Bellgowan, & Martin, 2010; Striem-Amit, Wang, Bi, & Caramazza, 2018; Wang, Conder, Blitzer, & Shinkareva, 2010; Zahn et al., 2007). Intriguingly, the anterior temporal lobe (ATL) is a brain region that has been broadly implicated in these semantic networks (for reviews see Lambon Ralph, Jefferies, Patterson, & Rogers, 2017; Xu, He, & Bi, 2017). While the ATL has been found to be composed of various "fine-grained" structures, such as those

Xiaosha Wang and Bijun Wang contributed equally to this study.

having sensitivity to different input modalities (Skipper, Ross, & Olson, 2011; Visser & Lambon Ralph, 2011) and different connectivity profiles (Binney, Parker, & Lambon Ralph, 2012; Jackson, Hoffman, Pobric, & Lambon Ralph, 2016), the organizing principle of various semantic dimensions has been a central issue in understanding the mechanisms of semantic processing in this area. When studying these specific semantic dimensions, other semantically relevant dimensions tend not to be held constant. This practice raises the question of whether multiple semantic dimensions are localized in the same ATL region and are driven by the same mechanisms, or whether the ATL contains different clusters showing sensitivity to different semantic dimensions. Here, we focus on the social-related semantic dimension as a testing case for this general issue.

It has been shown that semantic judgment of social word pairs (e.g., words describing human characteristics, such as "honor-brave") elicits stronger activations than those not typically or distinctively in reference to humans (e.g., "trainable-ridden") in the superior ATL, along with other regions, such as the posterior temporal and inferior parietal regions (Binney, Hoffman, & Lambon Ralph, 2016; Lin et al., 2018; Zahn et al., 2007). One dimension that may underlie at least some of the ATL preferences for the so-called social semantics is emotional valence, which tended to be confounded in previous studies. In one set of social/nonsocial words developed by Zahn and colleagues and repeatedly used in several studies (Binney et al., 2016; Ross & Olson, 2010; Zahn et al., 2007), social words were associated with positive (e.g., "honor") or negative (e.g., "impolite") feelings, whereas valence information was not mentioned for nonsocial words. The ATL social effect may not be affected by the polarity of valence, as it is found in both positive and negative concepts (Zahn et al., 2007), but it is unknown whether it is actually driven by the presence of emotional valence.

The confound of emotional valence in the ATL social effect is problematic especially because independent evidence suggests the involvement of the ATL in valence processing of words (Crosson et al., 1999; Ethofer et al., 2006; Kuchinke et al., 2005), but see Citron, Gray, Critchley, Weekes, & Ferstl, 2014; Hamann & Mao, 2002). The potential dissociation of social and valence processing in the ATL is also supported by recent anatomical and functional connectivity studies that parcellated the temporal pole (TP, the anterior portion of the ATL) into subregions connecting with regions involved in social and emotional processing (Fan et al., 2014; Pascual et al., 2015). One study reported that the left ATL responded to social/emotional, social, and object sentences in descending order (Mellem, Jasmin, Peng, & Martin, 2016). However, the three conditions also varied by other confounding variables (e.g., social content and concreteness ratings between the social/emotional and other conditions; unmatched valence between the social and object conditions), rendering the results difficult to interpret.

In this study, we first examined the effects of sociality, valence, and their potential interactions in the ATL using a 2 (social/nonsocial) × 2 (valenced/neutral) factorial design in an fMRI experiment. Note that social knowledge has been very broadly defined, from the mere presence of persons (Mellem et al., 2016; Norris, Chen, Zhu, Small, & Cacioppo, 2004), to the biographical information of specific persons (Simmons et al., 2010; Wang et al., 2017), and to socially interactive behaviors or properties (Zahn et al., 2007). Here, we focused on a specific type of "social" words, that is, those whose referents are meaningful in the context of interpersonal interactions (Binder et al., 2016; Lin, Bi, Zhao, Luo, & Li, 2015), to explicitly address the aspect of social interactions and to avoid the further confounding of additional semantic dimensions across conditions. We then tested the relationship between these dimensions and the well-documented abstractness preference in the ATL (Binder, Desai, Graves, & Conant, 2009; Wang et al., 2010), given the discussion about whether the abstractness preference is in fact driven by sociality and/or valence (Kousta, Vigliocco, Vinson, Andrews, & Del Campo, 2011; Zahn et al., 2007). Both the left and right ATL were of interest in this study, given the previous evidence of bilateral ATL involvement in social and emotional processing (Olson, McCoy, Klobusicky, & Ross, 2013; Pobric, Ralph, & Zahn, 2016; Rice, Ralph, & Hoffman, 2015). Whole-brain analyses, as well as resting-state functional connectivity analyses seeding from the ATL clusters with potential different functionalities, were further carried out to better understand the extent to which these clusters were indeed associated with the brain networks for the corresponding functionality (Lambon Ralph et al., 2017; Passingham, Stephan, & Kötter, 2002; Simmons et al., 2010). A relatively high spatial resolution (2 mm^3) multi-band fMRI sequence was used to better reveal the potential fine-scale effects.

2 | MATERIALS AND METHODS

2.1 | Participants

Twenty-three healthy college students (11 males; mean age 22.17 years, ranging from 19 to 29 years) participated in the fMRI experiment. The students were all right-handed, native Chinese speakers, and had normal or corrected-to-normal vision. The study was approved by the Human Subject Review Committee at Peking University, and all participants provided informed consent. One subject was excluded from data analysis because of a possible arachnoidal cyst in the right frontal lobe.

2.2 | Experimental design

We adopted a 2 × 2 factorial design with four concreteness-matched conditions of relatively abstract words: Social valenced (S+V+, e.g., "honor"), social neutral (S+V−, e.g., "duty"), nonsocial valenced (S−V+, e.g., "miracle"), and nonsocial neutral (S−V−, e.g., "content"). We included an additional condition of concrete object words (e.g., "spoon") to test the relationship between sociality/valence and general abstractness effects. For stimulus selection, we collected ratings of 633 two-character Chinese nouns on the following three properties: Sociality (how often the meaning of a noun involves an interaction between people (Binder et al., 2016; Lin et al., 2015), 1 = never, 7 = always), valence (1 = negative, 4 = neutral, 7 = positive), and concreteness (1 = very abstract; 7 = very concrete). We recruited

26, 33, and 31 college students for the above ratings, respectively, and computed the mean ratings for each word. Triplets were then generated with words from the same conditions, each consisting of one probe word and two choice words with one semantically related with the probe (target) and the other semantically unrelated (distractor).

The final stimulus set included 100 triplets, 20 triplets per condition. Triplet examples, ratings, and word frequency are provided in Table 1. The three words in each triplet were always from the same semantic condition except for some choice words (≤4). Some probe or target words were repeated as distractor words in other triplets. The numbers of words repeated were comparable among conditions (S+V + = 8, S+V− = 10, S−V+ = 7, S−V− = 6, Object = 8). A full list of the stimuli can be found in the Appendix.

Sociality ratings were matched for the two social and the two nonsocial conditions (Bonferroni-corrected *p*s = 1, post hoc Bonferroni tests following one-way analysis of variance [ANOVA], same below), with the social conditions being significantly more social than the nonsocial conditions (*p*s < .001). Under valenced conditions, half of the triplets were positive (valence ratings ≥5), and the other half of the triplets negative (valence ratings ≤3). Valence ratings were matched between the two neutral conditions and between positive words and between negative words in the two valenced conditions (independent-samples *t* tests, *p*s ≥ .12). The four abstract conditions were matched on concreteness (*p*s = 1) and were significantly more abstract and more social than object words (*p*s < .001), which were similarly neutral with the two abstract neutral conditions (*p*s = 1). All conditions were matched on the number of strokes (*p*s ≥ .326).

triplet level (i.e., values were averaged for the three words in a triplet). Finally, to rule out the potential differences in task difficulty among conditions, we recruited 19 college students in a pilot behavioral experiment and ensured that the five conditions were judged with comparable accuracy and reaction time (RT; *p*s ≥ .679).

2.3 | fMRI procedure

Task fMRI data were collected in a block-design paradigm in two runs. Each trial started with a 500 ms fixation cross, followed by a word triplet presented for 3,500 ms, with a probe word (e.g., "honor") displayed at the top, and two choice words (arranged horizontally) at the bottom (e.g., "fame" and "friendship"). Words were presented in black "Song" bold, 36-point sized font on a gray background, with a viewing distance of 1.1 m. Participants were asked to decide which of the choices was more semantically related to the probe by pressing a button corresponding to each choice with the right index or middle finger. There were five trials in each block (lasting 20 s) and 20 blocks (4 per condition) in each run. A 20-s fixation block followed every five word blocks, and a 12-s fixation period appeared at the beginning of each run (lasting 8 min 12 s). These procedures were implemented using E-prime 2. Each triplet appeared once in a run, and the same triplets were used in the two runs, with stimulus order and choice word locations shuffled. The order of conditions was counterbalanced within and across runs. The run order was counterbalanced across subjects.

One subject's behavioral data were excluded from the analysis because 31% of her responses were not recorded. Her neuroimaging data were included in the analysis because her accuracies were high for the trials to which she responded (94.2 and 98.6% for the two runs), suggesting a high level of vigilance.

Additionally, all subjects participated in an emotional localizer run (Barch et al., 2013; Hariri, Tessitore, Mattay, Fera, & Weinberger, 2002) to functionally localize emotion-related voxels in the amygdala for resting-state functional connectivity analyses (see below; note that the results were similar when the amygdala was defined anatomically). The task consisted of two conditions, namely, geometric shapes and emotional faces, and the subjects decided which of two shapes/faces presented at the bottom was identical to the shape/face presented at the top. The faces had either positive (happy) or negative (angry, fearful, sad, or disgust) expressions, which were selected from the Chinese affective picture system (Bai, Ma, & Huang, 2005). Shapes, positive faces, and negative faces were presented in blocks (20 s) of five trials (3,000 ms; interstimulus interval = 1,000 ms). There were eight face blocks alternated with eight shape blocks in the run (5 min 40 s).

2.4 | fMRI data acquisition

MRI data were collected on a 3 T MAGNETOM Prisma MR scanner (Siemens, Erlangen, Germany) with a 64-channel head–neck coil at the Centre for MRI Research, Peking University. High-resolution functional images were acquired using a multi-band echo-planar sequence (repetition time (TR) = 2000 ms, echo time (TE) = 30 ms, flip angle (FA) = 90°, field of view (FOV) = 224 mm × 224 mm, matrix size = 112 × 112, 62 axial slices, slice thickness = 2.0 mm, voxel size = 2 × 2 × 2 mm, multi-band factor = 2). High-resolution three-dimensional T1-weighted images were acquired using the magnetization-prepared rapid gradient-echo sequence (TR = 2,530 ms, TE = 2.98 ms, inversion time = 1,100 ms, FA = 7°, FOV = 256 mm × 224 mm, matrix size = 224 × 256, interpolated to 448 × 512, 192 sagittal slices, slice thickness = 1.0 mm, voxel size = 0.5 × 0.5 × 1 mm).

2.5 | fMRI data preprocessing

The images were preprocessed using SPM12 (Wellcome Trust Center for Neuroimaging, London, UK, http://www.fil.ion.ucl.ac.uk/spm/software/spm12/). For each participant's data, the first five volumes of each functional run were deleted, and the remaining images were corrected for head motion, spatially normalized to the Montreal Neurological Institute (MNI) space via the unified segmentation procedure (resampling into 2 × 2 × 2 mm voxel size) and smoothed with a Gaussian kernel of 6 mm full width at half maximum (FWHM). No participants showed excessive head movement (<1.08 mm or 1.36°).

2.6 | fMRI data analysis

For the first-level analysis, in a general linear model (GLM) preprocessed functional images were modeled with five regressors in each run, one per condition (S+V+, S+V−, S−V+, S−V−, and object), convolved with the canonical hemodynamic response function (HRF). The GLM also included six head motion parameters and a global mean predictor of each run. The high-pass filter was set at 128 s. After model estimation, whole-brain contrast images of each condition versus baseline were calculated for each subject. In addition, the contrast of S−V− > Object was computed to localize brain regions of abstractness, which was chosen to rule out the potential confounding effects of sociality and valence.

For the second-level analysis, a flexible factorial design was performed with sociality and valence as the within-subject factors. The contrasts of interest were the main effect of sociality [(S+V+ & S+V−) > (S−V+ & S−V−)], the main effect of valence [(S+V+ & S−V+) > (S+V− & S−V−)], and the sociality × valence interaction in two directions [((S+V+) – (S−V+)) > ((S + V−) – (S−V−)); ((S+V+) – (S−V+)) < ((S+V−) – (S−V−))]. One-sample *t*-test was used for the second-level analysis of the beta-weight images of the S−V− > Object.

To control for the potential influence of word frequency, we constructed a regressor containing the frequency per trial (i.e., frequency values were averaged across the three words), convolved it with the canonical HRF, and then included the frequency regressor in the original GLM as a nuisance covariate.

2.7 | ATL definition

Following the discussions about the boundaries of the ATL and TP in previous studies (Olson et al., 2013; Rice et al., 2015), we used an

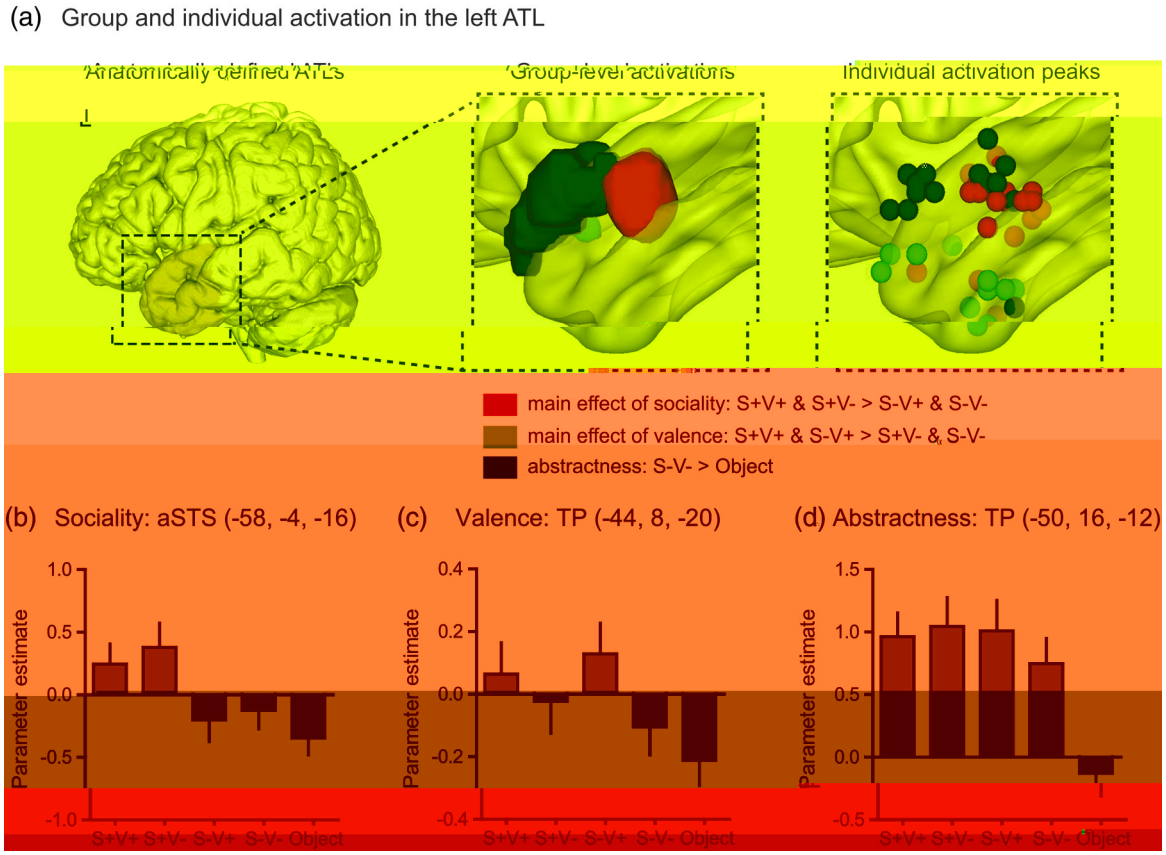

FIGURE 1 Localization of the functional subregions in the left ATL. (a) Left: A bilateral ATL mask was anatomically defined according to the Harvard–Oxford atlas. Only the left hemisphere is shown. Middle: Significant activation in the left ATL. Activation maps were thresholded at voxelwise $p < .001$, cluster-level FWE-corrected $p < .05$ for the main effect of sociality (red) and abstractness (blue) and cluster size ≥10 voxels for the main effect of valence (green), within the ATL mask. Right: Peak voxels in the left ATL in individual subjects showing the main effects of sociality (red) and valence (green), and abstractness (blue). Individual activation was thresholded at voxelwise $p < .01$, cluster size ≥10 voxels, within the ATL mask. (b–d) Bar graphs show the mean beta values per condition in a 6-mm-radius spherical ROI centered on the peak voxel of clusters in (b) the main effect of sociality, (c) the main effect of valence, and (d) the general abstractness effect. Error bars denote the standard error of the mean. S+V+, social valenced; S + V–, social neutral; S–V+, nonsocial valenced; S–V–, nonsocial neutral. L, left. Brain results are displayed using Mango (Research Imaging Institute, UTHSCSA, San Antonio, TX, available at http://ric.uthscsa.edu/mango/mango.html) and BrainNet viewer (Xia & He, 2013). No significant activations were observed in the right ATL after the cluster-level correction and the results at the threshold of voxelwise $p < .001$, cluster size ≥10 voxels were presented in Figure S2 [Color figure can be viewed at wileyonlinelibrary.com]

anatomical ATL mask covering the anterior portion of the temporal lobe (Figure 1a, left panel). The mask was defined according to the Harvard-Oxford Atlas (probability threshold > 0.2; Xu et al., 2018) as the union set of six subregions in both hemispheres (anterior to the line $y = -24$ along the ventral surface and $y = -14$ along the lateral surface in the MNI space): The temporal pole, the anterior superior temporal gyrus, the anterior middle temporal gyrus, the anterior inferior temporal gyrus, the anterior temporal fusiform cortex, and the anterior parahippocampal gyrus. The mask contained 9,706 voxels in total.

Given the magnetic susceptibility artifact in the ATL, we calculated the temporal signal-to-noise ratio (tSNR) maps for each subject by dividing the mean of smoothed time series in each voxel by its standard deviation in each run and averaging the tSNR across all runs (Murphy, Bodurka, & Bandettini, 2007). Figure S1 shows the mean tSNR map across all of the subjects. In the ATL, the tSNR values were comparable with previous studies (Hoffman, Binney, & Lambon Ralph, 2015; Simmons et al., 2010) and indicated acceptable coverage.

2.8 | Statistical analysis

The behavioral data (RT and accuracy) in the scanner were compared among the four abstract conditions (S+V+, S+V–, S–V+, and S–V–) using repeated-measures ANOVA with sociality and valence as the within-subject factors. The comparisons between the object and abstract conditions were carried out using paired t tests, followed by Bonferroni correction.

For neuroimaging data, activation maps were thresholded at voxelwise $p < .001$, FWE-corrected cluster-level $p < .05$ (based on cluster size), in the ATL mask or in the whole-brain volume. Note that Table 2 also reports nonsignificant regions thresholded at voxelwise $p < .001$, cluster size ≥10 voxels, following previous studies on social and valence effects in words (Crosson et al., 1999; Kuchinke et al., 2005; Zahn et al., 2007).

For regions surviving the cluster-level correction, to further visualize their activation profiles to different word conditions and to understand the relative specificity to the target contrast, we extracted the beta

TABLE 2 Activations within and outside the anterior temporal lobes (voxelwise $p < .001$, cluster size ≥10 voxels)

Cluster name (BA)	Cluster extent (voxels)	Peak *F*/*t* value	Maxima MNI coordinates		
			x	*y*	*z*

values of each condition versus the baseline from a spherical region of interest (ROI, radius = 6 mm, centering on the peak voxel of the cluster, 123 voxels) in individual subjects. We then performed repeated-measures ANOVA on these beta values, with sociality and valence as the within-subject factors. We did not report the contrast used to localize the cluster to avoid circularity (Poldrack, 2007).

2.9 | Resting-state data and functional connectivity analysis

To understand how the ATL subregions that show sociality, valence, and abstractness are intrinsically connected with the rest of the brain, we computed their resting-state functional connectivity (RSFC) using a dataset of 144 right-handed healthy young participants (data from Yang et al., 2017). All subjects provided written informed consent and the study was approved by the Institutional Review Board of the State Key Laboratory of Cognitive Neuroscience and Learning, Beijing Normal University. Image acquisition and preprocessing were previously described in detail (Yang et al., 2017). Briefly, participants were asked to stay awake and to rest with their eyes closed during the resting-state scan (lasting 6 min 40 s). The preprocessing steps included the removal of the first 10 volumes, slice timing, motion correction, spatial normalization into the MNI space using unified segmentation (resampling voxel size was $3 \times 3 \times 3$ mm), linear trend removal, bandpass filtering (0.01–0.1 Hz), spatial smoothing (6 mm FWHM Gaussian kernel) and regression of nuisance variables (including six rigid head motion parameters, the global signal, the white matter signal, and the cerebrospinal fluid signal).

Seed-based functional connectivity maps were calculated with the Resting-State fMRI Data Analysis Toolkit (Song et al., 2011, http://www.restfmri.net). Seed ROIs were obtained by creating spheres (radius: 6 mm, 33 voxels) around the peak voxel identified in the task neuroimaging analysis. For each subject, a whole-brain functional connectivity map for a given ROI was generated by correlating the mean time series of the seed ROI with the time series of every other voxel in the brain. The resulting *r*-maps were Fisher-*z* transformed and averaged across subjects to produce a group-level functional connectivity map, which was transformed back to an *r*-map and thresholded at 0.25 to illustrate the strong positive connections (Buckner et al., 2009; Liang, Zou, He, & Yang, 2013; Yeo et al., 2011). Considering the ongoing debate on the global signal regression in the RSFC computation (Murphy & Fox, 2017), we repeated our analyses without global signal regression and found similar RSFC patterns (Figure S4A). To identify the seed-specific functional connectivity patterns, we also performed a partial correlation analysis for a specific seed, that is, by including the time courses of the other two seeds as nuisance variables (Striem-Amit et al., 2016).

the ATL areas involved in word valence processing in previous studies adopting similar statistical thresholds (Ethofer et al., 2006; Kuchinke et al., 2005).

When restricting the valence effect to nonsocial words (i.e., S−V+ vs. S−V−), we found only one cluster in the left ATL with the same peak coordinates (peak t = 4.56; 25 voxels) as above, which indicates that the valence effect here was dissociable from sociality.

Sociality × valence interaction

No regions were found to be significant for this interaction in both directions in the ATL even at a lenient threshold of voxelwise $p < .001$, cluster size ≥10 voxels.

Individual subject analysis

Our results thus far indicated the dissociation between social and valence effects in the ATL at the group level without significant interaction; while the main effect of sociality activated the left aSTS, the main effect of valence activated small clusters in the bilateral TPs. To test whether the dissociation was reliable at the individual level, we localized these effects in each subject (at the threshold of voxelwise $p < .01$, cluster size ≥10 voxels) and examined the overlap (i.e., conjunction) among sociality, valence, and interaction effects.

In the left ATL, the main effect of sociality was observed in 18 subjects and the main effect of valence was observed in 11 subjects. The two effects overlapped in only one subject (10 out of 33 social voxels) and were also dissociated in spatial locations (Figure 1a, right panel). For the eight subjects with both effects in the left ATL, their social peaks (mean *xyz* (± standard deviations, SD): −57 (± 13), −5 (± 5), −16 (± 11)) were significantly more posterior and dorsal to their valence peaks (mean *xyz* (± SD): −50 (± 6), 8 (± 11), −31 (± 5); *y*-axis: paired t_7 = 3.127, p = .017; *z*-axis: paired t_7 = 3.449, p = .011). A sociality × valence interaction ([(S+V+) − (S−V+)] > [(S+V−) − (S−V−)]) was observed in five subjects, and the interaction in the opposite direction was observed in 10 subjects. Importantly, in subjects showing both interactions and main effects, the interactions did not affect the interpretations of the main effects, as the overlap of these effects were observed in only one to two subjects out of 22 subjects.

In the right ATL, activation was observed in 9 subjects for the main effect of sociality, in 13 subjects for the main effect of valence, and in 11 subjects for the interaction. As shown in Figure S2B, these individual peaks were scattered throughout the right ATL, which is consistent with the nonsignificant group-level effects. A spatial overlap between the two main effects (sociality and valence) was found in only one subject (47 out of 53 social voxels), and an overlap between main effects and interactions was found in only two subjects.

Taken together, these individual results confirmed the dissociation of sociality from valence effects in the left ATL and the nonsignificant group-level effects in the right ATL.

Effects outside the ATL

We performed exploratory whole-brain analyses for sociality, valence, and their interactions (Table 2) and here reported regions surviving the cluster-level correction. In addition to the left aSTS, the main effect of sociality was also found in a cluster including the angular gyrus, the posterior middle temporal gyrus, and the middle occipital gyrus in the left hemisphere (termed as the occipito-temporo-parietal junction [OTPJ] for convenience, Figure 2a). This region showed deactivations to all of the abstract conditions, with social words showing weaker deactivations than nonsocial words in both valenced and neutral words (paired $t_{21} \geq 2.452$, $p \leq .023$). A sociality × valence

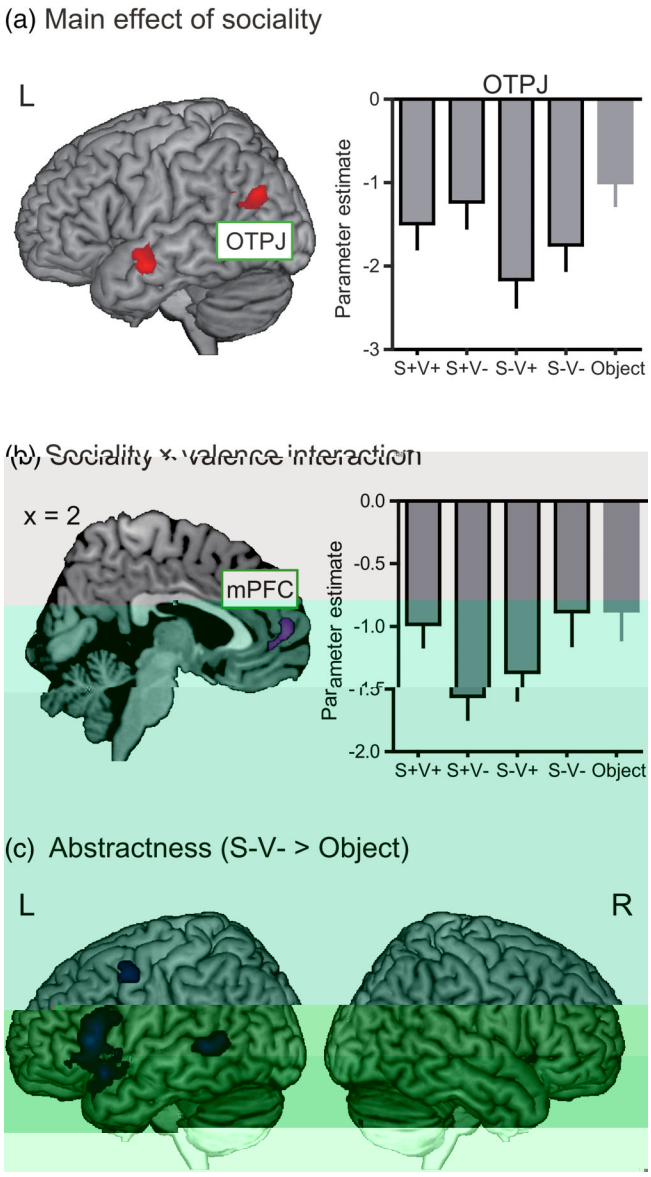

FIGURE 2 Whole-brain activation results. (a) Main effect of sociality, (b) the sociality × valence interaction, and (c) abstractness. Activation maps were thresholded at voxelwise $p < .001$, FWE-corrected cluster-level $p < .05$. Bar graphs show the mean beta values per condition from a 6-mm-radius spherical ROI centered on the peak voxel of each cluster. OTPJ, occipito-temporo-parietal junction; mPFC, medial prefrontal cortex; S+V+, social valenced; S+V−, social neutral; S−V+, nonsocial valenced; S−V−, nonsocial neutral. L, left; R, right. Brain results are displayed using MRIcron (available at www.mccauslandcenter.sc.edu/mricro/mricron/index.html) [Color figure can be viewed at wileyonlinelibrary.com]

interaction was observed in the middle medial prefrontal cortex (mPFC, Figure 2b). This region was also deactivated by all of the abstract conditions, showing no main effects of sociality or valence (Fs [1, 21] ≤ 1.098, ps ≥ .307). The interaction was driven by the opposite social effect for valenced and neutral words: Deactivations were stronger for nonsocial than social conditions in valenced words (paired t_{21} = 2.432, p = .024), and the pattern was reversed in neutral words (paired t_{21} = −2.807, p = .011).

3.2.2 | The effects of abstractness in semantic processing in the ATL

We further examined the relationship between the social/valence effects and the general abstractness preference in the ATL. Abstract words consistently evoked a higher activation than concrete words in the left superior ATL (Binder et al., 2009; Wang et al., 2010). However, previous studies showing the abstractness effect might have included social words and/or words with emotional valence (Kousta et al., 2011; Skipper et al., 2011; Zahn et al., 2007). Here, we first localized the ATL subregion that showed a general abstractness preference and then examined its response profile to the four abstract conditions.

Social and valence effects in the "abstractness ATL subregion"

We localized regions that showed abstractness effects using the S−V− versus Object contrast, which was chosen to rule out the potential confounding effects of sociality and valence. In the ATL, this contrast produced significant activation in the left superior TP and anterior superior temporal gyrus (peak *xyz*: −50, 16, −12; Figure 1a, blue cluster, and Table 2). This region also showed stronger activations to other abstract conditions relative to objects (Figure 1d, paired ts ≥ 7.357, ps ≤ 3.0×10^{-7}). An omnibus F test revealed no significant difference among the four abstract conditions (F [3, 63] = 2.150, p = .103). Abstractness was found in a small cluster in the right TP, but it did not survive the cluster-level correction (Figure S2A and D; peak t = 4.19; peak *xyz*: 50, 16, −18; 18 voxels).

Individual subject analysis

We verified the dissociation of abstractness, sociality, and valence at the individual level. In the left ATL, abstractness was localized (voxelwise p < .01, cluster size ≥10 voxels) in 15 subjects. For the 13 subjects with both abstractness and social effects in the left ATL (Figure 1a, right panel), the abstractness peaks (mean *xyz* (± SD): −57 (± 3), 7 (± 10), −11 (± 3)) were significantly more anterior and dorsal to the social peaks (mean *xyz* (± SD): −56 (± 11), −4 (± 8), −18 (± 9); *y*-axis: paired t_{12} = 3.680, p = .003; *z*-axis: paired t_{12} = 2.405, p = .033). For the seven subjects with both abstractness and valence effects in the left ATL, the abstractness peaks (mean *xyz* (± SD): −56 (± 4), 3 (± 11), −13 (± 12)) were more lateral and dorsal than the valence peaks (mean *xyz*: −45 (± 9), 4 (± 11), −31 (± 5); *x*-axis: paired t_6 = 3.916, p = .008; *z*-axis: paired t_6 = 3.098, p = .021). Conjunction analyses showed that abstractness and social effects overlapped in four subjects and that abstractness and valence did not overlap in individual subjects, consistent with their dissociation at the group level. In the right ATL, 13 subjects exhibited abstractness effects with their peaks scattered throughout the superior ATL (Figure S2B), consistent with the nonsignificant effect at the group level.

Abstractness outside the ATL

Whole-brain analysis (Figure 2c and Table 2) of the S−V− versus Object contrast showed that the left superior ATL cluster was a subpeak of a larger cluster with peak coordinates in the left inferior frontal gyrus. Significant activations were also observed in the left posterior middle temporal gyrus, the left precentral gyrus extending to the middle frontal gyrus, the right insula, and the right cerebellum.

3.2.3 | Validation analysis: Controlling for the potential effect of word frequency

Words in the four abstract conditions were carefully matched on subjective familiarity and behavioral responses, not on word frequency for valenced and neutral words. Here, we performed a validation analysis to control for the potential influence of word frequency on fMRI results by including word frequency in the GLM as a nuisance variable.

Previous fMRI studies observed word frequency effects in several brain regions including the left inferior frontal and occipito-temporal regions (Chee, Venkatraman, Westphal, & Siong, 2003; Hauk, Davis, & Pulvermüller, 2008; Schuster, Hawelka, Hutzler, Kronbichler, & Richlan, 2016), not in the ATL, which is the region of interest in the current study. In this validation analysis, increasing word frequency was significantly associated with higher activation in the left inferior frontal gyrus and with lower activation in the bilateral occipital–temporal regions (Figure S3A and Table S1), but not in the ATL, even at a lenient threshold of voxelwise p < .001, cluster size ≥10 voxels. The results of sociality, sociality × valence interaction, and abstractness were similar to the main analyses (Figure S3B–E and Table S1). The main effects of valence, which may be particularly subject to frequency effects, were found in three small clusters in the left ATL in this analysis, with two clusters similar to the clusters reported in the main analyses and the third cluster (peak *x y z*: −46, 8, −30, 54 voxels) similar to those previously reported in the literature (Ethofer et al., 2006; Kuchinke et al., 2005).

3.2.4 | Resting-state functional connectivity patterns of distinct ATL subregions

To test whether the different ATL clusters that showed sociality, valence, and abstractness are associated with different brain networks of the corresponding functions, we examined their resting-state functional connectivity (RSFC) patterns in 144 young healthy subjects. The regions showing the strong positive connections with the ATL clusters are displayed in Figure 3a and Table S2 (group-averaged connectivity strength R > 0.25). The social aSTS ROI (center voxel: −58, −4, −16) functionally connected with the homologous ATL in the right hemisphere and the bilateral precuneus/posterior cingulate gyri,

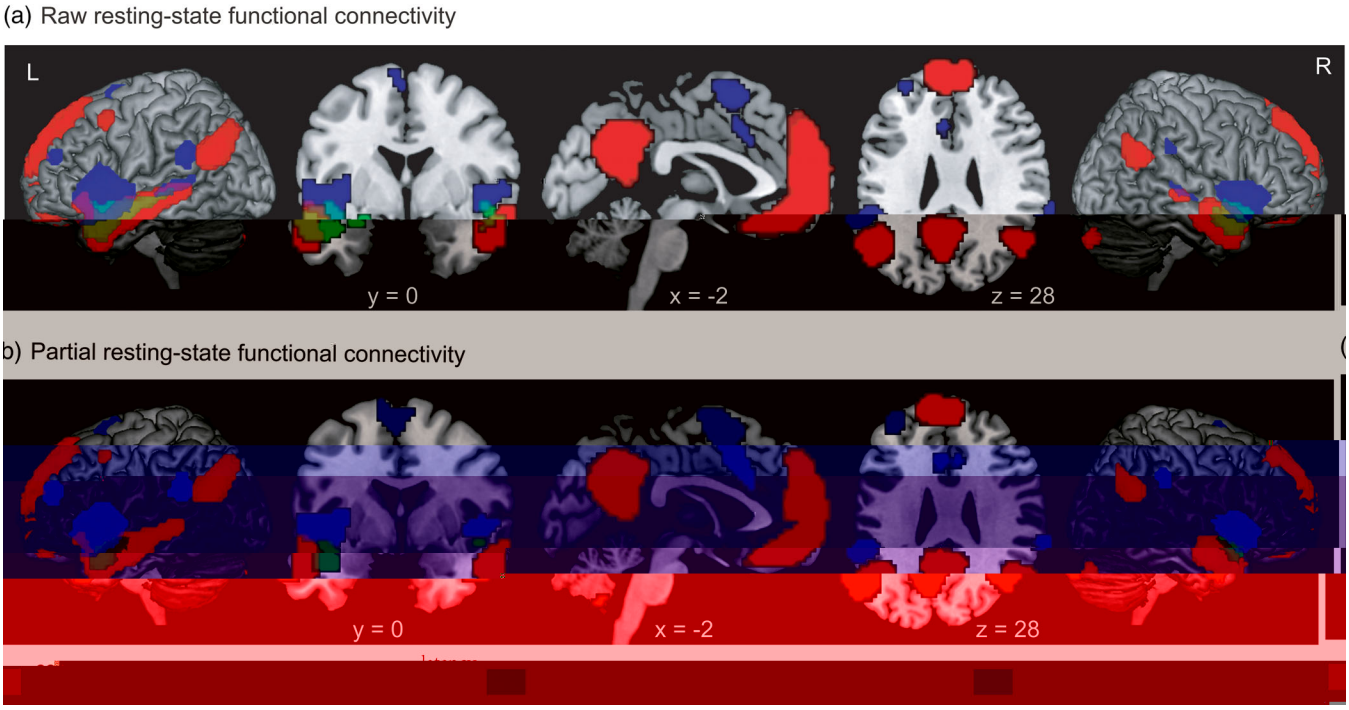

FIGURE 3 Resting-state functional connectivity maps of the ATL subregions for sociality, valence, and abstractness. Functional connectivity was computed by a direct correlation between the time course of a seed region with that of each voxel in the brain (a) or by a partial correlation analysis, in which the time courses of the remaining two ATL subregions were controlled for (b). Mean connectivity maps are shown here at a threshold of 0.25, cluster size >10 voxels. L, left; R, right [Color figure can be viewed at wileyonlinelibrary.com]

medial frontal cortex/anterior cingulate gyri, and the posterior temporal and inferior parietal regions (termed as the aSTS-network). The valence ROI (center voxel: −44, 8, −20) was functionally connected with the bilateral ATLs extending to the insula and inferior frontal gyrus, and the left amygdala. The abstractness ROI (center voxel: −50, 16, −12) was functionally connected with the bilateral inferior frontal gyri, posterior superior temporal gyri, supramarginal gyri, middle temporal gyri, and supplementary motor areas. Given the regional adjacency and overlapping connectivity patterns between these ROIs, to examine the region-specific connections, we carried out partial correlations when computing connectivity for one seed region with the time courses of the two remaining ATL subregions as covariates. The connectivity maps remained largely unaffected except that there was less overlap in the temporal lobe surrounding the seed regions (Figure 3b).

The RSFC maps in Figure S4 show connectivity patterns thresholded at the conventional threshold in the RSFC analysis (voxelwise FWE-corrected $p < .05$, cluster size >10 voxels). While the social and abstractness clusters showed similar connectivity patterns (with greater spatial extents), the valence cluster connected with many other regions, including some regions in the aSTS-network (with smaller spatial extents than regions connected with the social ROI) and the bilateral amygdala (Figure S4B). Interestingly, for region-specific connections (Figure S4C), the connections of the social ROI with the aSTS-network regions persisted, as did the connections of the valence ROI with the bilateral amygdala, which is indicative of the respective connections of the two regions with different networks.

To further understand the relationship between the ATL and the regions involved in general emotional processing, we specifically tested the RSFC of the three ATL subregions with the emotion-sensitive regions in the bilateral amygdala defined by an independent nonverbal emotional localizer. In agreement with previous reports (Barch et al., 2013; Hariri et al., 2002), our functional emotional localizer, contrasting emotional faces with geometric shapes, elicited robust activations (Figure S5A) of the bilateral amygdala (left amygdala, peak t = 10.02, peak *xyz*: −22, −6, −16, 65 voxels; right amygdala, peak t = 11.49, peak *xyz*: 20, 0, −16, 143 voxels; voxelwise FWE-corrected $p < .05$) and the ventral temporal cortex, which are likely due to visual perceptual processing of faces given that the localizer did not control for basic face processing. Comparison of the RSFC between the bilateral amygdala clusters and the three ATL subregions showed that the (verbal) valence ATL cluster, compared with the social and abstractness clusters, was more strongly connected with the bilateral amygdala regions (paired $t_{143} > 4.060$, $ps < .001$, Figure S5B). These results were similar when the amygdala was defined anatomically.

4 | DISCUSSION

The ATL is a crowded brain area for semantic processing, involved in multiple types of semantic information, which need to be carefully disentangled. Considering the confound of emotional valence in previous studies of social words in the ATL, in this study, we orthogonally manipulated these dimensions in a 2 × 2 factorial design to examine

the influence of sociality and emotional valence on the ATL activity in semantic processing of abstract words at the 2 mm^3 fMRI resolution scale. We found that the left ATL processed sociality and emotional valence in different locations and without significant interactions. Social words evoked stronger activations in the left aSTS compared with nonsocial words, with high consistency across individuals. The valence effects were much less clear, tending to activate a small cluster in the superior portion of the left TP at the group level, with large individual variations. These two regions are functionally and anatomically distinct from a more general "abstractness" ATL cluster, which was not modulated by the social or valence contents of the abstract words. These three ATL subregions, although anatomically close to each other, were intrinsically connected with different functional networks. Below, we discuss these regions/dimensions in turn.

4.1 | Sociality effects in the left anterior superior temporal sulcus

The left aSTS showed stronger activations to social words than to nonsocial words, regardless of whether the words were valenced ("honor" > "miracle") or neutral ("duty" > "reason"). The social effect cannot be attributed to emotional valence, concreteness, familiarity, word frequency, or task difficulty, which were carefully matched between social and nonsocial conditions. As described in the Introduction, "sociality" has been operationalized in different ways in the literature and roughly falls into two aspects: Person-related (with or without referents about interactions with other persons), or interpersonal interactions (without reference to specific persons). We explicitly chose items entailing the latter to be more in line with the conventional understanding of "social". The majority of the 120 social words in our experiment were social products, rules, or properties that emerged from interpersonal interactions (e.g., "honor" or "duty"), and the observed social effects likely reflected general social knowledge pertaining to interactions among animate entities. Only four words in our stimuli referred to social groups (3 S+V+ words: talents, tyrant, and gangster; 1 S+V− word: civilians). Thus, the social effects in our blocked design are unlikely to be driven by social group effects as previously reported (Contreras, Banaji, & Mitchell, 2012).

What is the relationship between the social semantics preferred by the left aSTS found here and those involved in social interactions? Several recent studies have examined the neural correlates of real-life social interactions (e.g., Eisenberger, Inagaki, Muscatell, Haltom, & Leary, 2011; Hughes & Beer, 2013; Schindler, Kruse, Stark, & Kissler, 2019), contrasting the same words in different social contexts (perspective taking; i.e., subtracting out the words' general semantic activation), and reported widespread activations in regions such as the medial prefrontal or anterior cingulate cortex depending on the specific contrast of interest, but not the left aSTS. Our experiments here, being interested in the representation of social information in general word semantics, contrasted different words (with or without social knowledge) in neutral contexts. Therefore, the brain regions activated in our study and in social processing studies could be different due to different experimental tasks and contrasts. The left aSTS found here has not been reported in experiments using nonverbal person-related stimuli (e.g., human voices, faces, or biological motion; Deen, Koldewyn, Kanwisher, & Saxe, 2015) or cartoons depicting social interactions (Centelles, Assaiante, Nazarian, Anton, & Schmitz, 2011; Isik, Koldewyn, Beeler, & Kanwisher, 2017; but see Ross & Olson, 2010), either, and seems to be located posteriorly to the TP area that stores person-related semantic knowledge (Ross & Olson, 2012; Simmons et al., 2010; Wang et al., 2017; Wang, Peelen, Han, Caramazza, & Bi, 2016). On the other hand, the regions intrinsically connected with the left aSTS anatomically overlap with the default mode network (Yeo et al., 2011), which has been associated with a range of cognitive tasks that are related to loosely defined social processing: Autobiographical memory retrieval, prospection, theory of mind (Spreng, Mar, & Kim, 2008), social interaction perception (Centelles et al., 2011; Iacoboni et al., 2004), and human-specific interaction (Schindler et al., 2019). Taken together, it is possible that this aSTS region processes social semantics that are abstracted away from perceptual aspects (e.g., the human form or motion) of interpersonal interactions, but are tightly related to regions preferentially responding to social interaction, together forming a network for social processing. Indeed, clinical case studies have documented both dissociations (Feinstein, Adolphs, Damasio, & Tranel, 2011) and associations (Zahn et al., 2009) between semantic knowledge and real-life social/emotional behaviors.

The lack of sociality effects in the right ATL is worth further discussion given that previous studies have observed the involvement of the right ATL in social processing. For instance, clinical studies in patients with frontotemporal lobar degeneration (FTD) suggest that right ATL integrity is crucial in social/emotional behaviors (Edwards-Lee et al., 1997; Rankin, Kramer, Mychack, & Miller, 2003). Such results might not be driven by semantic impairments. Zahn and colleagues explicitly examined social word processing in FTD patients and found that at the group level patients with right ATL hypometabolism were more impaired on social words than on animal function (nonsocial) words (Zahn et al., 2009). Close scrutiny of individual cases, however, shows that right ATL hypometabolism is not necessary or sufficient to cause social word selective impairment. In the neuroimaging studies, the activation of the right ATL to social semantics was not shown in some studies (the current study, Ross & Olson (2010), and the social vs. animal function word contrast in Binney et al. (2016), but see Zahn et al. (2007) and the social vs. matched abstract word contrast in Binney et al. (2016)), and what drives such a discrepancy remains to be resolved. Note that transcranial magnetic stimulation (TMS) to both the left and right ATL in healthy subjects significantly impaired social word processing (Pobric et al., 2016), and it is not clear whether both are necessary or the results are driven by the intrinsic functional connectivity between the bilateral ATLs. That is, while the left ATL is consistently implicated in processing social- and emotional-word meanings across neuroimaging and TMS studies, the effects of the right ATL are much less robust.

4.2 | Valence effects in the temporal poles

Unlike the robust, consistent effects for social semantics, an emotional valence effect was found in small clusters in the superior portion of the bilateral TPs, which did not survive the cluster-level correction at the group level and showed large individual variations anatomically. The neural correlates of emotional valence effects have been extensively studied using nonverbal stimuli (e.g., emotional faces), which revealed consistent involvement of the frontolimbic regions, such as the amygdala, but inconsistent

Y.B.), and the 111 Project (BP0719032). We thank Professor Yong He for sharing the resting-state data, and Dr. Ella Striem-Amit and Huichao Yang for helpful discussion.

CONFLICT OF INTERESTS

The authors declare no competing financial interests.

DATA AVAILABILITY STATEMENT

The data that support the findings of this study are available from the corresponding author upon reasonable request.

ORCID

Xiaosha Wang https://orcid.org/0000-0002-2133-8161
Yanchao Bi https://orcid.org/0000-0002-0522-3372

REFERENCES

Bai, L., Ma, H., & Huang, Y. (2005). The development of native Chinese affective picture system—A pretest in 46 college students. *Chinese Mental Health Journal*, *19*, 719–722.

Barch, D. M., Burgess, G. C., Harms, M. P., Petersen, S. E., Schlaggar, B. L., Corbetta, M., … Van Essen, D. C. (2013). Function in the human connectome: Task-fMRI and individual differences in behavior. *NeuroImage*, *80*, 169–189. https://doi.org/10.1016/j.neuroimage.2013.05.033

Barsalou, L. W., & Wiemer-Hastings, K. (2005). Situating abstract concepts. In D. Pecher & R. Zwaan (Eds.), *Grounding cognition: The role of perception and action in memory, language, and thought*. New York: Cambridge University Press.

Bi, Y., Wei, T., Wu, C., Han, Z., Jiang, T., & Caramazza, A. (2011). The role of the left anterior temporal lobe in language processing revisited: Evidence from an individual with ATL resection. *Cortex*, *47*, 575–587. https://doi.org/10.1016/j.cortex.2009.12

Binder, J., Westbury, C., McKiernan, K., Possing, E., & Medler, D. (2005). Distinct brain systems for processing concrete and abstract concepts. *Journal of Cognitive Neuroscience*, *17*, 905–917.

Binder, J. R., Conant, L. L., Humphries, C. J., Fernandino, L., Simons, S. B., Aguilar, M., & Desai, R. H. (2016). Toward a brain-based componential semantic representation. *Cognitive Neuropsychology*, *3294*, 1–45. https://doi.org/10.1080/02643294.2016.1147426

Binder, J. R., Desai, R. H., Graves, W. W., & Conant, L. L. (2009). Where is the semantic system? A critical review and meta-analysis of 120 functional neuroimaging studies. *Cerebral Cortex*, *19*, 2767–2796. https://doi.org/10.1093/cercor/bhp055

Binney, R. J., Hoffman, P., & Lambon Ralph, M. A. (2016). Mapping the multiple graded contributions of the anterior temporal lobe representational hub to abstract and social concepts: Evidence from distortion-corrected fMRI. *Cerebral Cortex*, *26*, 4227–4241. https://doi.org/10.1093/cercor/bhw260

Binney, R. J., Parker, G. J. M., & Lambon Ralph, M. A. (2012). Convergent connectivity and graded specialization in the rostral human temporal lobe as revealed by diffusion-weighted imaging probabilistic tractography. *Journal of Cognitive Neuroscience*, *24*, 1998–2014. https://doi.org/10.1162/jocn_a_00263

Buckner, R. L. L., Sepulcre, J., Talukdar, T., Krienen, F. M. M., Liu, H., Hedden, T., … Johnson, K. A. A. (2009). Cortical hubs revealed by intrinsic functional connectivity: Mapping, assessment of stability, and relation to Alzheimer's disease. *The Journal of Neuroscience*, *29*, 1860–1873. https://doi.org/10.1523/JNEUROSCI.5062-08.2009

Centelles, L., Assaiante, C., Nazarian, B., Anton, J. L., & Schmitz, C. (2011). Recruitment of both the mirror and the mentalizing networks when observing social interactions depicted by point-lights: A neuroimaging study. *PLoS One*, *6*, e15749. https://doi.org/10.1371/journal.pone.0015749

Chee, M. W. L., Venkatraman, V., Westphal, C., & Siong, S. C. (2003). Comparison of block and event-related fMRI designs in evaluating the word-frequency effect. *Human Brain Mapping*, *18*, 186–193. https://doi.org/10.1002/hbm.10092

Citron, F. M. M. (2012). Neur.200eur.., vity.

Feinstein, J. S., Adolphs, R., Damasio, A., & Tranel, D. (2011). The human amygdala and the induction and experience of fear. *Current Biology*, *21*, 34–38. https://doi.org/10.1016/j.cub.2010.11.042

Friederici, A. D., Chomsky, N., Berwick, R. C., Moro, A., & Bolhuis, J. J. (2017). Language, mind and brain. *Nature Human Behaviour*, *1*, 713–722. https://doi.org/10.1038/s41562-017-0184-4

Gernsbacher, M. A. (1984). Resolving 20 years of inconsistent interactions between lexical familiarity and orthography, concreteness, and polysemy. *Journal of Experimental Psychology. General*, *113*, 256–281.

Hamann, S., & Mao, H. (2002). Positive and negative emotional verbal stimuli elicit activity in the left amygdala. *Neuroreport*, *13*, 15–19.

Hariri, A. R., Tessitore, A., Mattay, V. S., Fera, F., & Weinberger, D. R. (2002). The amygdala response to emotional stimuli: A comparison of faces and scenes. *NeuroImage*, *17*, 317–323.

Hauk, O., Davis, M. H., & Pulvermüller, F. (2008). Modulation of brain activity by multiple lexical and word form variables in visual word recognition: A parametric fMRI study. *NeuroImage*, *42*, 1185–1195. https://doi.org/10.1016/j.neuroimage.2008.05.054

Hertrich, I., Dietrich, S., & Ackermann, H. (2016). The role of the supplementary motor area for speech and language processing. *Neuroscience and Biobehavioral Reviews*, *68*, 602–610. https://doi.org/10.1016/j.neubiorev.2016.06.030

Hoffman, P., Binney, R. J., & Lambon Ralph, M. A. (2015). Differing contributions of inferior prefrontal and anterior temporal cortex to concrete and abstract conceptual knowledge. *Cortex*, *63*, 250–266. https://doi.org/10.1016/j.cortex.2014.09.001

Hughes, B. L., & Beer, J. S. (2013). Protecting the self: The effect of social-evaluative threat on neural representations of self. *Journal of Cognitive Neuroscience*, *25*, 613–622. https://doi.org/10.1162/jocn_a_00343

Iacoboni, M., Lieberman, M. D., Knowlton, B. J., Molnar-Szakacs, I., Moritz, M., Throop, C. J., & Fiske, A. P. (2004). Watching social interactions produces dorsomedial prefrontal and medial parietal BOLD fMRI signal increases compared to a resting baseline. *NeuroImage*, *21*, 1167–1173. https://doi.org/10.1016/j.neuroimage.2003.11.013

Isik, L., Koldewyn, K., Beeler, D., & Kanwisher, N. (2017). Perceiving social interactions in the posterior superior temporal sulcus. *Proceedings of the National Academy of Sciences of the United States of America*, *114*, E9145–E9152. https://doi.org/10.1073/pnas.1714471114

Jackson, R. L., Hoffman, P., Pobric, G., & Lambon Ralph, M. A. (2016). The semantic network at work and rest: Differential connectivity of anterior temporal lobe subregions. *The Journal of Neuroscience*, *36*, 1490–1501. https://doi.org/10.1523/JNEUROSCI.2999-15.2016

Kousta, S. T., Vigliocco, G., Vinson, D. P., Andrews, M., & Del Campo, E. (2011). The representation of abstract words: Why emotion matters. *Journal of Experimental Psychology. General*, *140*, 14–34. https://doi.org/10.1037/a0021446

Kuchinke, L., Jacobs, A. M., Grubich, C., Võ, M. L. H., Conrad, M., & Herrmann, M. (2005). Incidental effects of emotional valence in single word processing: An fMRI study. *NeuroImage*, *28*, 1022–1032. https://doi.org/10.1016/j.neuroimage.2005.06.050

Lambon Ralph, M. A., Jefferies, E., Patterson, K., & Rogers, T. T. (2017). The neural and computational bases of semantic cognition. *Nature Reviews. Neuroscience*, *18*, 42–55. https://doi.org/10.1038/nrn.2016.150

Liang, X., Zou, Q., He, Y., & Yang, Y. (2013). Coupling of functional connectivity and regional cerebral blood flow reveals a physiological basis for network hubs of the human brain. *Proceedings of the National Academy of Sciences of the United States of America*, *110*, 1929–1934. https://doi.org/10.1073/pnas.1214900110

Lin, N., Bi, Y., Zhao, Y., Luo, C., & Li, X. (2015). The theory-of-mind network in support of action verb comprehension: Evidence from an fMRI study. *Brain and Language*, *141*, 1–10. https://doi.org/10.1016/j.bandl.2014.11.004

Lin, N., Wang, X., Xu, Y., Wang, X., Hua, H., Zhao, Y., & Li, X. (2018). Fine subdivisions of the semantic network supporting social and sensory-motor semantic processing. *Cerebral Cortex*, *28*, 2699–2710. https://doi.org/10.1093/cercor/bhx148

Lindquist, K. A., Satpute, A. B., Wager, T. D., Weber, J., & Barrett, L. F. (2016). The brain basis of positive and negative affect: Evidence from a meta-analysis of the human neuroimaging literature. *Cerebral Cortex*, *26*, 1910–1922. https://doi.org/10.1093/cercor/bhv001

Mellem, M. S., Jasmin, K. M., Peng, C., & Martin, A. (2016). Sentence processing in anterior superior temporal cortex shows a social-emotional bias. *Neuropsychologia*, *89*, 217–224. https://doi.org/10.1016/j.neuropsychologia.2016.06.019

Murphy, K., Bodurka, J., & Bandettini, P. A. (2007). How long to scan? The relationship between fMRI temporal signal to noise ratio and necessary scan duration. *NeuroImage*, *34*, 565–574. https://doi.org/10.1016/j.neuroimage.2006.09.032

Murphy, K., & Fox, M. D. (2017). Towards a consensus regarding global signal regression for resting state functional connectivity MRI. *NeuroImage*, *154*, 169–173. https://doi.org/10.1016/j.neuroimage.2016.11.052

during virtual feedback processing. *Cognitive, Affective, & Behavioral Neuroscience*, *19*, 239–252. https://doi.org/10.3758/s13415-018-00660-5

Schuster, S., Hawelka, S., Hutzler, F., Kronbichler, M., & Richlan, F. (2016). Words in context: The effects of length, frequency, and predictability on brain responses during natural Reading. *Cerebral Cortex*, *26*, 3889–3904. https://doi.org/10.1093/cercor/bhw184

Sergerie, K., Chochol, C., & Armony, J. L. (2008). The role of the amygdala in emotional processing: A quantitative meta-analysis of functional neuroimaging studies. *Neuroscience and Biobehavioral Reviews*, *32*, 811–830. https://doi.org/10.1016/j.neubiorev.2007.12.002

Simmons, W. K., Reddish, M., Bellgowan, P. S. F., & Martin, A. (2010). The selectivity and functional connectivity of the anterior temporal lobes. *Cerebral Cortex*, *20*, 813–825. https://doi.org/10.1093/cercor/bhp149

Skipper, L. M., Ross, L. A., & Olson, I. R. (2011). Sensory and semantic category subdivisions within the anterior temporal lobes. *Neuropsychologia*, *49*, 3419–3429. https://doi.org/10.1016/j.neuropsychologia.2011.07.033

Song, X., Dong, Z., Long, X., Li, S., Zuo, X., Zhu, C., … Zang, Y. (2011). REST: A toolkit for resting-state functional magnetic resonance imaging data processing. *PLoS One*, *6*, e25031. https://doi.org/10.1371/journal.pone.0025031

Spreng, R. N., Mar, R. A., & Kim, A. S. N. (2008). The common neural basis of autobiographical memory, prospection, navigation, theory of mind, and the default mode: A quantitative meta-analysis. *Journal of Cognitive Neuroscience*, *21*, 489–510. https://doi.org/10.1162/jocn.2008.21029

Striem-Amit, E., Almeida, J., Belledonne, M., Chen, Q., Fang, Y., Han, Z., … Bi, Y. (2016). Topographical functional connectivity patterns exist in the congenitally, prelingually deaf. *Scientific Reports*, *6*, 1–13. https://doi.org/10.1038/srep29375

Striem-Amit, E., Wang, X., Bi, Y., & Caramazza, A. (2018). Neural representation of visual concepts in people born blind. *Nature Communications*, *9*, 5250. https://doi.org/10.1038/s41467-018-07574-3

Sun, H. L., Huang, J. P., Sun, D. J., Li, D. J., & Xing, H. B. (1997). Introduction to language corpus system of modern Chinese study. In M. Y. Hu (Ed.), *Paper collection for the fifth world Chinese teaching symposium* (pp. 459–466). Beijing: Peking University Publishers.

Tzourio-Mazoyer, N., Landeau, B., Papathanassiou, D., Crivello, F., Etard, O., Delcroix, N., … Joliot, M. (2002). Automated anatomical labeling of activations in SPM using a macroscopic anatomical parcellation of the MNI MRI single-subject brain. *NeuroImage*, *15*, 273–289. https://doi.org/10.1006/nimg.2001.0978

Visser, M., & Lambon Ralph, M. A. (2011). Differential contributions of bilateral ventral anterior temporal lobe and left anterior superior temporal gyrus to semantic processes. *Journal of Cognitive Neuroscience*, *23*, 3121–3131. https://doi.org/10.1162/jocn_a_00007

Wager, T. D., Phan, K. L., Liberzon, I., & Taylor, S. F. (2003). Valence, gender, and lateralization of functional brain anatomy in emotion: A meta-analysis of findings from neuroimaging. *NeuroImage*, *19*, 513–531.

Wang, J., Conder, J. A., Blitzer, D. N., & Shinkareva, S. V. (2010). Neural representation of abstract and concrete concepts: A meta-analysis of neuroimaging studies. *Human Brain Mapping*, *31*, 1459–1468. https://doi.org/10.1002/hbm.20950

Wang, X., Peelen, M. V., Han, Z., Caramazza, A., & Bi, Y. (2016). The role of vision in the neural representation of unique entities. *Neuropsychologia*, *87*, 144–156. https://doi.org/10.1016/j.neuropsychologia.2016.05.007

Wang, X., Wu, W., Ling, Z., Xu, Y., Fang, Y., Wang, X., … Bi, Y. (2018). Organizational principles of abstract words in the human brain. *Cerebral Cortex*, *28*, 4305–4318. https://doi.org/10.1093/cercor/bhx283

Wang, Y., Collins, J. A., Koski, J., Nugiel, T., Metoki, A., & Olson, I. R. (2017). Dynamic neural architecture for social knowledge retrieval. *Proceedings of the National Academy of Sciences of the United States of America*, *114*, E3305–E3314. https://doi.org/10.1073/pnas.1621234114

Xia, M., & He, Y. (2013). BrainNet viewer: A network visualization tool for human brain connectomics. *PLoS One*, *8*, e68910. https://doi.org/10.1371/journal.pone.0068910

Xu, Y., He, Y., & Bi, Y. (2017). A tri-network model of human semantic processing. *Frontiers in Psychology*, *8*, 1538. https://doi.org/10.3389/fpsyg.2017.01538

Xu, Y., Wang, X., Wang, X., Men, W., Gao, J.-H., & Bi, Y. (2018). Doctor, teacher, and stethoscope: Neural representation of different types of semantic relations. *The Journal of Neuroscience*, *38*, 3303–3317. https://doi.org/10.1523/JNEUROSCI.2562-17.2018

Yang, H., Lin, Q., Han, Z., Li, H., Song, L., Chen, L., … Bi, Y. (2017). Dissociable intrinsic functional networks support noun-object and verb-action processing. *Brain and Language*, *175*, 29–41. https://doi.org/10.1016/j.bandl.2017.08.009

Yeo, B. T., Krienen, F. M., Sepulcre, J., Sabuncu, M. R., Lashkari, D., Hollinshead, M., … Buckner, R. L. (2011). The organization of the human cerebral cortex estimated by intrinsic functional connectivity. *Journal of Neurophysiology*, *106*, 1125–1165. https://doi.org/10.1152/jn.00338.2011

Zahn, R., Moll, J., Iyengar, V., Huey, E. D., Tierney, M., Krueger, F., & Grafman, J. (2009). Social conceptual impairments in frontotemporal lobar degeneration with right anterior temporal hypometabolism. *Brain*, *132*, 604–616. https://doi.org/10.1093/brain/awn343

Zahn, R., Moll, J., Krueger, F., Huey, E. D., Garrido, G., & Grafman, J. (2007). Social concepts are represented in the superior anterior temporal cortex. *Proceedings of the National Academy of Sciences of the United States of America*, *104*, 6430–6435. https://doi.org/10.1073/pnas.0607061104

SUPPORTING INFORMATION

Additional supporting information may be found online in the Supporting Information section at the end of this article.

How to cite this article: Wang X, Wang B, Bi Y. Close yet independent: Dissociation of social from valence and abstract semantic dimensions in the left anterior temporal lobe. *Hum Brain Mapp*. 2019;1–18. https://doi.org/10.1002/hbm.24735

APPENDIX

Word triplets used in this study (Chinese words and English translations, organized by condition).

Social valenced (S+V+) triplets						
	Probe		Target		Distractor	
1	荣誉	Honor	功名	Fame	友情	Friendship
2	榜样	Role model	模范	Good example	真情	True feelings

(Continues)

3		Responsibility		Conscience	民	Democracy
4		Credibility		Reputation		Etiquette
5		Morality		Cultivation		Achievement
6		Kindness		Charity		Credibility
7		Love		Predestinated relationship		Vacation
8		Festival		Ceremony		Predestinated relationship
9		Wedding		Honeymoon		Talents
10		Family		Marriage		Honor
11		Rumor		Falsehood		Funeral
12		Lie		Fraud		Public outrage
13		Crime		Horrible crime		Wile
14	歧	Disagreement	盾	Conflict		Hearsay
15		Hatred		Hostility	歧	Disagreement
16		Despotism		Tyrant		Heresy
17		Beravement		Deathday		Debt
18		Violence		Gangster		Falsehood
19		Dispute		Debt		Excuse
20		Conspiracy		Wile		Deadlock
Social neutral (S+V) triplets						
	Probe		Target		Distractor	
1		Authority		Representative		Society
2		Team		Group		Privacy
3		Role		Identity	民	Situation of the people
4		Status		Price/wealth of somebody		Public opinion
5		Income		Economy		Message
6		Opinion		Argument		Group
7		Life		Privacy		Working performance
8	百	Civilians	民	Situation of the people		Duty
9		Performance		Treatment		Military affairs
10		Discipline		Institution		Focus
11		Media		Subject of talk		International
12		Relationship		Network		Liberal arts
13		Order	法治	Rule by law		Statement
14		Duty		Title		Subject of talk
15		News		Public opinion		Labor
16		Agreement	盟	Alliance		Impression
17		Business		Deal		Character
18		Descent		Family		Market
19		Society		Doctrine		Descent
20		Supply and demand		Market	法治	Rule by law
Nonsocial valenced (S V+) triplets						
	Probe		Target		Distractor	
1		Vitality		Youth		Skill
2		Verve		Gloss		Nutrient
3		Environmental protection		Scenery		Dawn
4		Knowledge		Intelligence		Passion
5		Heaven		God		Direction
6		Ability		Endowment		Dreaminess

(Continues)

7	□分	Nutrient	沃土	Fertile soil	心灵	Spirit
8	时机	Opportunity	运气	Fortune	神韵	Verve
9	本领	Capability	技能	Skill	□心	Determination
10	奇迹	Marvel	魔力	Magic	□源	Resource
11	障碍	Obstacle	困难	Hardness	绝□	Fatal disease
12	干旱	Drought	灾	Flood	阴霾	Haze
13	□□	Disease	伤□	Pain	破烂	Raggedness
14	缺陷	Defect	残□	Disability	难度	Difficulty
15	晦气	Misfortune	霉运	Bad luck	瑕□	Flaw
16	挫折	Frustration	磨难	Suffering	伤残	Injury
17	弊端	Drawback	缺点	Weakness	死亡	Death
18	瑕□	Flaw	毛□	Fault	干旱	Drought
19	死亡	Death	绝□	Fatal disease	错误	Mistake
20	过失	Negligence	代价	Price	糟粕	Dross
Nonsocial neutral (S−V−) triplets						
	Probe		Target		Distractor	
1	系数	Coefficient	□式	Formula	技术	Technology
2	格□	Framework	整体	Entirety	句法	Syntax
3	特征	Characteristic	性□	Property	片段	Fragment
4	物理	Physics	数学	Mathematics	灵魂	Soul
5	标	Coordinate	位置	Location	意思	Meaning
6	概念	Concept	定义	Definition	故事	Story
7	逻辑	Logic	结论	Conclusion	品□	Trait
8	品□	Trait	风格	Style	实体	Entity
9	模	Model	理论	Theory	神话	Mythology
10	比例	Scale	数量	Amount	软件	Software
11	状态	State	□势	Trend	间距	Spacing
12	区别	Distinction	□异	Difference	信息	Information
13	真相	Truth	事实	Reality	方面	Aspect
14	□容	Content	含义	Implication	指南	Guide
15	思路	Train of thought	想法	Idea	世□	World
16	□象	Phenomenon	原理	Principle	体系	System
17	原因	Reason	结果	Result	状态	State
18	□境	Environment	卫□	Sanitation	□势	Trend
19	命运	Fate	□实	Reality	原理	Principle
20	数据	Data	信息	Information	真相	Truth
Object triplets						
	Probe		Target		Distractor	
1	筷子	Chopstick	勺子	Spoon	夹子	Clip
2	书包	Schoolbag	铅笔	Pencil	花瓶	Vase
3	项链	Necklace	手镯	Bracelet	耳机	Earphone
4	枕头	Pillow	靠垫	Cushion	插座	Plug-in
5	鼠标	Mouse	键盘	Keyboard	算盘	Abacus
6	毛□	Towel	牙刷	Toothbrush	书包	Schoolbag
7	粉笔	Chalk	板擦	Board eraser	眼	Glasses
8	鱼竿	Fishing rod	船桨	Quant	拖把	Mop
9	相机	Camera	胶卷	Film	枕头	Pillow
10	蜡烛	Candle	火柴	Match	吸管	Straw

(Continues)

11	圆规	Compasses	□子	Ruler	蜡烛	Candle
12	剪刀	Scissors	胶布	Adhesive tape	项链	Necklace
13	钥匙	Key	钱包	Wallet	手套	Glove
14	手链	Bracelet	戒指	Ring	相框	Photo frame
15	扫帚	Broom	拖把	Mop	刀	Sickle
16	水□	Kettle	杯子	Cup	雨伞	Umbrella
17	纽扣	Button	拉链	Zipper	粉笔	Chalk
18	信□	Envelope	邮票	Stamp	手镯	Bracelet
19	照片	Photo	相框	Photo frame	书本	Book
20	子	Hammer	铁钉	Nail	□盘	CD